JOURNAL OF MATERIALS SCIENCE 19 (1984) 3953–3966

Enthalpy relaxation behaviour of $(Fe, Co, Ni)_{75}Si_{10}B_{15}$ amorphous alloys upon low temperature annealing

A. INOUE, T. MASUMOTO
The Research Institute for Iron, Steel and Other Metals, Tohoku University, Sendai 980, Japan

H. S. CHEN
Bell Laboratories, Murray Hill, New Jersey 07974, USA

The effect of composition on the anneal-induced enthalpy relaxation for (Fe, Co, $Ni)_{75}Si_{10}B_{15}$ amorphous alloys was examined calorimetrically. Upon heating the sample annealed at temperatures well below T_g ($T_a < T_g - 150$ K), an excess endothermic reaction (enthalpy relaxation) occurs above the annealing temperature. The endothermic specific heat, ΔC_p, evolves in a continuous manner with annealing time. The change in the magnitude of ΔC_p with T_a is divided into two stages: a low-temperature stage which peaks at about $T_g - 150$ K and a high-temperature peak just below T_g. The activation energy, E_m, increases with the peak temperature of ΔC_p, T_m, from 2.29 to 3.15 eV for the low-temperature peak and from 4.40 to 4.96 eV for the high-temperature peak. The low-temperature endothermic reaction is attributed to local and medium range atomic rearrangements and the high-temperature reaction to the long-range cooperative atomic regroupings. The magnitude of the low-temperature ΔC_p is most pronounced for $(Fe–Co)_{75}Si_{10}B_{15}$, followed by $(Fe–Ni)_{75}Si_{10}B_{15}$, $(Co–Ni)_{75}Si_{10}B_{15}$, $Fe_{75}Si_{10}B_{15}$, $Co_{75}Si_{10}B_{15}$ and then $Ni_{75}Si_{10}B_{15}$. The reason for such a significant compositional effect of the enthalpy relaxation was investigated, based on the concept of distribution in relaxation time, which had been previously derived from the percolation theory, and was interpreted as due to the difference in the degree of local structure and compositional disorder in the as-quenched state; i.e. the higher the degree of short-range disorder (the larger the fraction of short relaxation time) the larger is the magnitude of the enthalpy relaxation ($\Delta H_{\sigma,endo}$). There existed a strong correlation between $\Delta H_{\sigma,endo}$ or ΔC_p and anneal-induced embrittlement tendency; the larger the $\Delta H_{\sigma,endo}$ and ΔC_p the larger is the embrittlement tendency. Such a strong correlation was interpreted based on the assumption that the internal strain which generated in the transition from as-quenched disordered state to a relaxed equilibrium state causes an enhancement of embrittlement tendency.

1. Introduction

Because an amorphous phase is structurally in the metastable state and thermodynamically in a non-equilibrium state, further heat-treatment to the amorphous phase results in structural relaxation which causes significant changes in physical, chemical and mechanical properties. It is therefore very important for scientific and technological points of view to clarify quantitatively the structural relaxation phenomenon of amorphous alloys. The structural relaxation behaviour was intensively investigated by measurement of internal friction

0022–2461/84 $03.00 + .12

[1–3], energy contribution [4, 5], atomic configuration [6, 7], ferromagnetic Curie point [5, 8–10], Young's modulus [11–13], electrical resistance [14, 15], superconducting critical temperature [16–19] and so forth. As a result, the existence of reversible and irreversible processes was confirmed and the possibility of two separate changes of topological and compositional short-range order was proposed [9].

More recently, it has been found [20–25] for a number of metal–metalloid type amorphous alloys such as Pd–Ni–(P or Si) and Fe–Ni–P–B–(Al) systems that the amorphous alloys annealed at temperatures well below the glass transition temperature (T_g) or crystallization temperature (T_x) exhibit an endothermic peak at a temperature slightly higher than the annealing temperature (T_a) and further heating results in the same exothermic reaction as that of the as-quenched sample. Based on such a new phenomenon, a new model for the mechanism of the structural relaxation has been proposed [22, 23]. The appearance of the endothermic peak implies that the enthalpy of an amorphous solid decreases, indicative of the increase in the stability of the amorphous structure upon annealing. A quantitative investigation on the enthalpy relaxation phenomenon is expected to bring a new and useful information on the origin of the changes in the physical properties of amorphous alloys described above upon structural relaxation as well as the mechanism of the structural relaxation. There is, however, no systematic information on the enthalpy relaxation for (Fe, Co, Ni)–Si–B amorphous alloys which are the most important alloy systems as industrial magnetic materials. The purpose of this paper is three-fold:

1. to clarify the effect of composition on the enthalpy relaxation behaviour for amorphous $(Fe, Co, Ni)_{75}Si_{10}B_{15}$ ternary and quaternary alloys annealed for different periods at various temperatures below T_g without causing crystallization;

2. to investigate its compositional effect based on the concept of distribution in relaxation time which had been previously proposed in the framework of a percolation theory [22, 23]; and

3. to examine the correlation between the enthalpy relaxation and the anneal-induced embrittlement.

2. Experimental methods

Amorphous ribbons of $Fe_{75}Si_{10}B_{15}$, $Co_{75}Si_{10}B_{15}$ and $Ni_{75}Si_{10}B_{15}$ ternary and $(Fe_{1-x}Co_x)_{75}Si_{10}B_{15}$, $(Fe_{1-x}Ni_x)_{75}Si_{10}B_{15}$ and $(Co_{1-x}Ni_x)_{75}Si_{10}B_{15}$ ($x = 0.25$, 0.50 and 0.75) quaternary alloys, typically 20 to 25 μm thick and 1 mm wide, were prepared by using a single-roller melt spinning method and confirmed to be amorphous by conventional X-ray diffractometer which used Cu$K\alpha$ radiation in combination with an X-ray monochrometer. The subscripts are assumed to be those of the unalloyed pure elements since the difference between weighed and chemically analysed compositions was less than 0.05 wt% for silicon and 0.10 wt% for boron. The apparent specific heat, C_p, was measured with a differential scanning calorimeter (Perkin–Elmer DSC-II). Care was taken to reduce the thermal drift by prewarming the calorimeter for at least 5 h in the temperature range of interest. The accuracy of the data was about 0.8 J mol^{-1} K^{-1} for the absolute C_p values, but was better than 0.4 J mol^{-1} K^{-1} for the relative C_p or ΔC_p measurements.

The as-quenched samples were subjected to annealing treatments at various temperatures below T_g (T_a = 500 to 700 K) for different periods (t_a = 1 to 200 h). Short-period anneals ($t_a \leqslant 60$ h) were performed directly inside the calorimeter while long-duration anneals (60 to 200 h) were performed in a well-controlled furnace after placing the encapsulated samples inside a vacuum-sealed quartz tube.

Following annealing treatment, the sample was thermally scanned at 40 K min^{-1} from 320 to 795 K to determine the C_p of the as-quenched or annealed sample. It was then cooled to 320 K, and reheated immediately to obtain the C_p data of the "reference" sample (i.e. the pre-conditioned sample without further low-temperature annealing). This test procedure is essential in order to eliminate any possible error that might result from the drift in the calorimeter due to the prolonged annealing time between the measurements. The change in the calorimeter behaviour with annealing was used to monitor the structural relaxation processes.

3. Results

3.1. General feature of $C_p(T)$ behaviour

The change in the thermograms of $(Fe_{0.5}Ni_{0.5})_{75}Si_{10}B_{15}$ amorphous alloys with annealing time t_a at T_a = 600 K and with annealing temperature, T_a, for t_a = 3 h is shown in Figs. 1 and 2, respectively. The C_p value of the as-quenched sample is

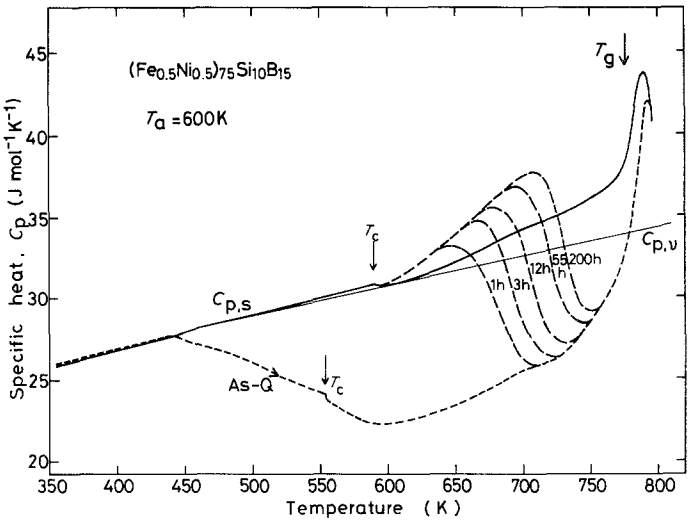

Figure 1 The thermograms of an amorphous $(Fe_{0.5}Ni_{0.5})_{75}Si_{10}B_{15}$ alloy subjected to anneals at 600 K for various periods from 1 to 200 h. The solid line represents the thermogram of the sample subjected to heating to 795 K.

about 25.7 J mol^{-1}K^{-1} near room temperature, being the same as that of $(Fe_{0.5}Ni_{0.5})_{75}P_{16}B_6Al_3$ alloy [21]. On subsequent heating, C_p begins to decrease, indicative of a structural relaxation at about 445 K, and shows a minimum value of about 22.5 J mol^{-1}K^{-1} in the vicinity of 590 K. With further increase in temperature, C_p increases gradually to about 750 K and then rapidly, indicative of a glass transition. The C_p of both the as-quenched (As-Q) and the reference ($C_{p,s}$) samples approaches the equilibrium liquid values above 795 K. Figs. 1 and 2 also show that the C_p value near room temperature is slightly lower for the reference sample than for the as-quenched sample. The change in the $C_p(T)$ behaviour of the $(Fe_{0.5}Ni_{0.5})_{75}Si_{10}B_{15}$ amorphous alloy upon continuous heating is very analogous to the previous results [20–25] for Pd–Ni–(P or Si) and Fe–Ni–P–B–Al amorphous alloys. The heating curve of the annealed sample shows a $C_p(T)$ behaviour which closely follows the C_p curve of the reference sample, $C_{p,s}$, up to each annealing temperature, and then exhibits an excess endotherm relative to the reference sample before merging with that of the as-quenched sample at a temperature below $T_g = 776$ K where T_g is defined as the point of inflection in the curve of C_p against T.

The significant feature of Figs. 1 and 2 may be summarized as:

1. the sample annealed at T_a shows an excess endothermic specific heat beginning at T_a, implying that the specific heat in the temperature range above T_a is dependent on the thermal history and consists of configurational contributions as well as

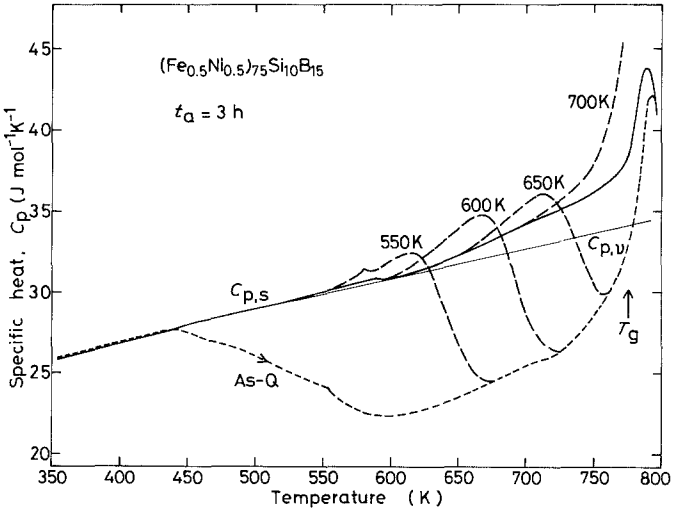

Figure 2 The thermograms of an amorphous $(Fe_{0.5}Ni_{0.5})_{75}Si_{10}B_{15}$ alloy subjected to anneals for 3 h at various temperatures from 550 to 700 K. The solid line represents the thermogram of the sample subjected to heating to 795 K.

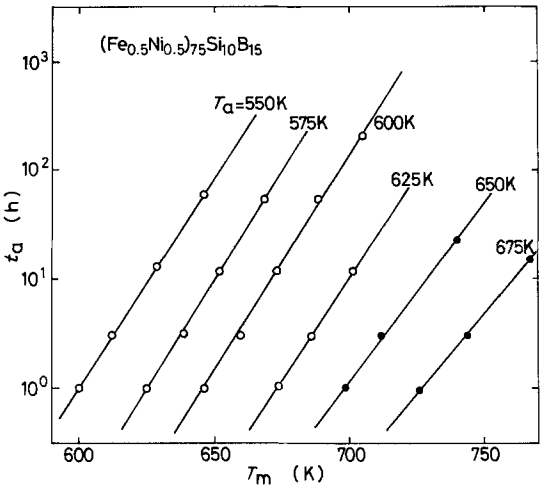

Figure 3 Variation of the $\Delta C_p = C_p - C_{p,v}$ peak temperature, T_m, as a function of annealing time, t_a, for an amorphous $(Fe_{0.5}Ni_{0.5})_{75}Si_{10}B_{15}$ alloy annealed at various temperatures from 550 to 675 K.

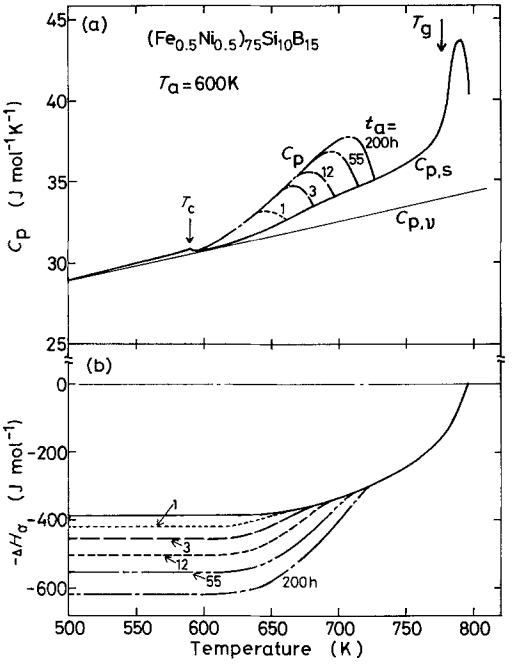

Figure 4 (a) The endothermic peak of an amorphous $(Fe_{0.5}Ni_{0.5})_{75}Si_{10}B_{15}$ alloy subjected to anneals at 600 K for various periods from 1 to 200 h. (b) The change in the configuration enthalpy $\Delta H_\sigma(T)$ corresponding to the appearance of the endothermic peak for an amorphous $(Fe_{0.5}Ni_{0.5})_{75}Si_{10}B_{15}$ alloy, where ΔH_σ (795 K) is set to zero.

those arising from purely thermal vibrations. Therefore, the vibrational specific heat, $C_{p,v}$, which was extrapolated from C_p values in the low-temperature region, $T \leqslant 550$ K, is a linear function of temperature such that

$$C_{p,v} = 30.0 + 2.2 \times 10^{-2}(T - 550)\,\mathrm{J\,mol^{-1}\,K^{-1}}. \quad (1)$$

However, the equilibrium specific heat of the supercooled liquid including the vibrational and configurational specific heat, $C_{p,e}$, was not determined owing to the high instability around T_g for the $(Fe_{0.5}Ni_{0.5})_{75}Si_{10}B_{15}$ amorphous alloy, evidence for which is given by the fact that a large exothermic peak due to crystallization appears at a temperature just above T_g ($\simeq$ 800 K);

2. if the annealing is performed at temperatures well below T_g ($T_a \leqslant 650$ K), it does not affect the glass transition process. This is indicated by the close overlap of C_p curves for the annealed and unannealed samples at temperatures below T_g;

3. the excess endothermic curves always begin to rise at T_a, being independent of annealing time. Furthermore, Fig. 3 shows that both the magnitude and the temperature of the endothermic peak tend to increase in proportion to the logarithm of the time (t_a);

4. the excess endothermic peak is recoverable while the exothermic broad peak is irrecoverable and the $C_p(T)$ curve of the annealed samples couples the recoverable endothermic and irrecoverable exothermic reaction. The strict separation of the relaxation process into chemical short-range order and topological short-range order is thought to be over simplified. It has been suggested that the recoverable relaxation arises from short-range localized relaxation in regions of the more or less rigid matrix while the irrecoverable structural relaxation results from the annihilation of various kinds of frozen-in "defects" [22, 26, 27].

The change in the configuration enthalpy, $\Delta H_\sigma(T)$, of the $(Fe_{0.5}Ni_{0.5})_{75}Si_{10}B_{15}$ amorphous alloy upon annealing at T_a for t_a was evaluated by paying attention to only the endothermic peak shown in Figs. 1 and 2, and the results are shown in Figs. 4 and 5. The hypothetical thermograms consisting of only the endothermic peak shown in Figs. 4a and 5a are thought to correspond to those of the annealed samples after thermal preconditioning at temperatures near T_g, even though measurement of the thermograms on thermally preconditioned samples was not performed in the present work, because almost all the amorphous alloys in the $(Fe, Co, Ni)_{75}Si_{10}B_{15}$ system are thermally

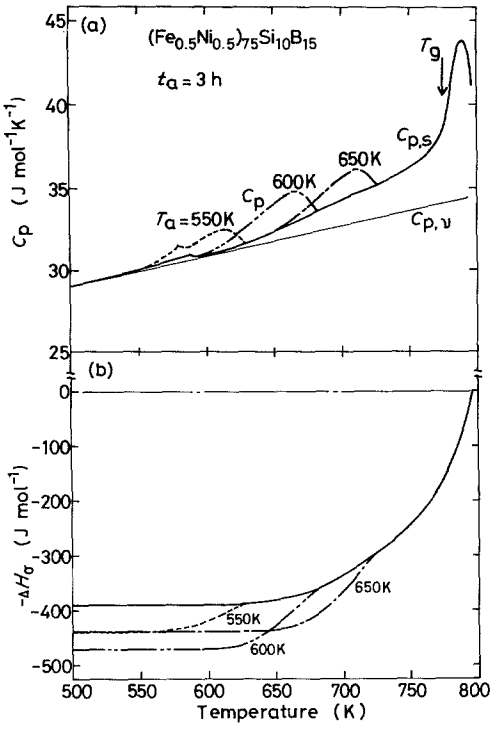

Figure 5 (a) The endothermic peak of an amorphous $(Fe_{0.5}Ni_{0.5})_{75}Si_{10}B_{15}$ alloy subjected to anneals for 3 h at various temperatures ranging from 550 to 650 K. (b) The change in the configuration enthalpy $\Delta H_\sigma(T)$ corresponding to the appearance of the endothermic peak for an amorphous $(Fe_{0.5}Ni_{0.5})_{75}Si_{10}B_{15}$ alloy, where ΔH_σ (795 K) is set to zero.

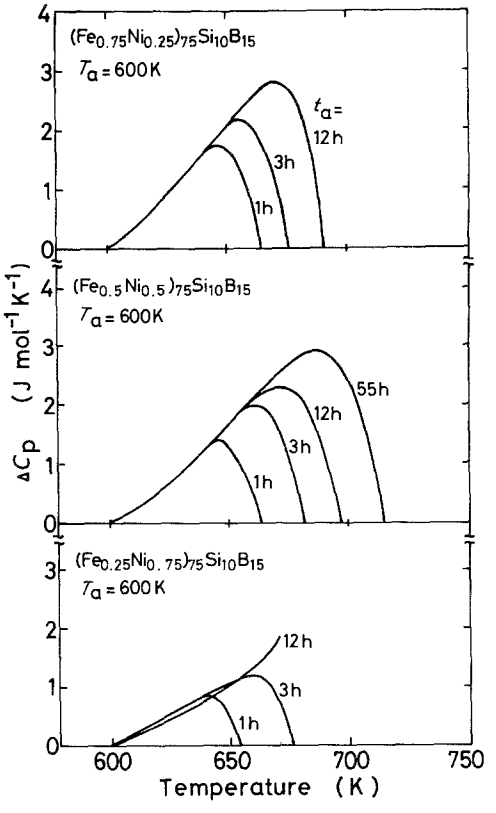

Figure 6 The differential specific heats, $\Delta C_p(T)$, between the reference and annealed samples for a series of $(Fe–Ni)_{75}Si_{10}B_{15}$ amorphous alloys subjected to anneals at 600 K for different periods from 1 to 55 h.

unstable, as seen from the fact that crystallization begins before the transition from amorphous solid to supercooled liquid. Here the configurational enthalpy at 795 K was taken to be the reference with $\Delta H_\sigma(795\,\text{K}) = 0$, and the relaxed configurational enthalpy $\Delta H_\sigma(T)$ was expressed by:

$$\Delta H_\sigma(T) = \int_{795}^{T} (C_p - C_{p,v})\,dT. \qquad (2)$$

As seen in the figures, the configurational enthalpy curve falls progressively with annealing time and annealing temperature, indicating that the low-temperature anneals stabilize the amorphous structure. With rising temperature, ΔH_σ of the annealed sample increases towards the reference value and merges with it before glass transition, implying that it is possible to recover the initial structure of the amporphous alloy without reheating above T_g. This feature differs significantly from the phenomenon [28–30] commonly observed for the amorphous materials on annealing in a temperature range slightly below T_g.

3.2. Compositional dependence of $\Delta C_p(T)$ and $\Delta H_{\sigma,\text{endo}}$ behaviours

With an aim to clarify the effect of composition on the magnitude of the enthothermic peak, the temperature dependence of the differences in C_p between the annealed ($T_a = 600$ K, $t_a = 1, 3, 12, 55$ h) and the reference states, $[\Delta C_p(T) = C_p(T) - C_{p,v}(T)]$ is shown in Fig. 6 for a series of $(Fe–Ni)_{75}Si_{10}B_{15}$ samples, in Fig. 7 for $(Fe–Co)_{75}Si_{10}B_{15}$, in Fig. 8 for $(Co–Ni)_{75}Si_{10}B_{15}$ and in Fig. 9 for $Fe_{75}Si_{10}B_{15}$ and $Co_{75}Si_{10}B_{15}$ alloys. The features of these figures may be noted as follows. Firstly, the magnitude of the ΔC_p increases in the order of Fe–Co > Fe–Ni > Ni–Co > Fe > Co systems, indicating that the enthalpy relaxation occurs more significantly for the quaternary alloys consisting of two kinds of mother metals than for the ternary alloys. Secondly, the magnitude for the quaternary alloys is greater for the alloys containing iron, indicating that the dissolution of iron enhances the degree of the enthalpy relaxation. Thirdly, the magnitude and temperature of the

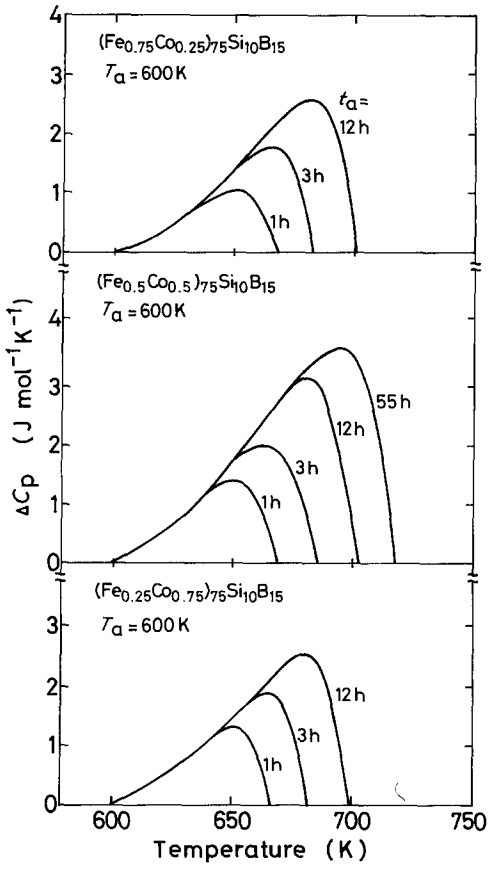

Figure 7 The differential specific heats, $\Delta C_p(T)$, between the reference and annealed samples for a series of $(Fe–Co)_{75}Si_{10}B_{15}$ amorphous alloys subjected to anneals at 600 K for different periods from 1 to 55 h.

ΔC_p peak increase with annealing time, t_a, in a continuous manner. As exemplified in Fig. 3 for $(Fe_{0.5}Ni_{0.5})_{75}Si_{10}B_{15}$ alloy, the peak temperature, T_m, varies linearly as the logarithm of t_a.

Fig. 10 shows the change in enthalpy relaxation as a function of annealing time at $T_a = 600\,K$ for the $(Fe_{0.5}Ni_{0.5})_{75}Si_{10}B_{15}$ and $(Fe_{0.5}Co_{0.5})_{75}Si_{10}B_{15}$ amorphous alloys exhibiting large enthalpy relaxation. The total enthalpy relaxed, $\Delta H_{\sigma,\mathrm{endo}}(T_a, t_a)$, is given by Equation 3,

$$\Delta H_{\sigma,\mathrm{endo}}(T_a, t_a) = \int_{T_a}^{T} \Delta C_p(T)\,dT \quad \text{for } \Delta C_p(T) \geqslant 0. \tag{3}$$

$\Delta H_{\sigma,\mathrm{endo}}(600\,K)$ of both the alloys increases with $(\ln t_a)^n$ ranging from 1 to 2. This linear to quadratic $\ln t_a$ dependence of $\Delta H_{\sigma,\mathrm{endo}}(600\,K)$ is expected, as both the magnitude and temperature of the ΔC_p peak increase with $\ln t_a$ (see Fig. 1), being

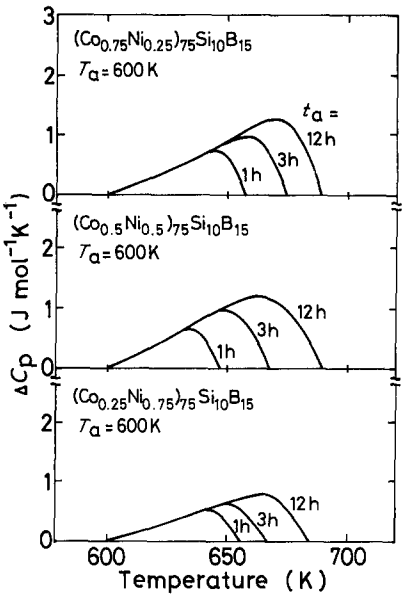

Figure 8 The differential specific heats, $\Delta C_p(T)$, between the reference and annealed samples for a series of $(Co–Ni)_{75}Si_{10}B_{15}$ amorphous alloys subjected to anneals at 600 K for different periods from 1 to 12 h.

the same as that by low-temperature annealing for $Pd_{48}Ni_{32}P_{20}$ alloy [22].

Fig. 11 shows the composition dependence of the maximum differential specific heat $\Delta C_{p,\max} = C_p - C_{p,\nu}$ and the enthalpy relaxation $\Delta H_{\sigma,\mathrm{endo}}$ during annealing at $T_a = 600\,K$ for different periods (t_a) for (Fe, Co, Ni)$_{75}$Si$_{10}$B$_{15}$ amorphous alloys. The $\Delta C_{p,\max}$ and $\Delta H_{\sigma,\mathrm{endo}}(600\,K)$ exhibit a maximum value around $x = 0.5$ Co for $(Fe_{1-x}Co_x)_{75}Si_{10}B_{15}$, around $x = 0.4$ Ni for $(Co_{1-x}Ni_x)_{75}Si_{10}B_{15}$, and around $x = 0.75$ Fe for $(Ni_{1-x}Fe_x)_{75}Si_{10}B_{15}$, and their maximum values

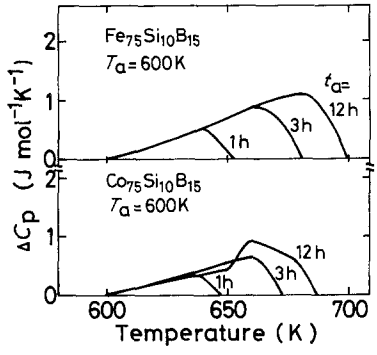

Figure 9 The differential specific heats, $\Delta C_p(T)$, between the reference and annealed samples for $Fe_{75}Si_{10}B_{15}$ and $Co_{75}Si_{10}B_{15}$ amorphous alloys subjected to anneals at 600 K for different periods from 1 to 12 h.

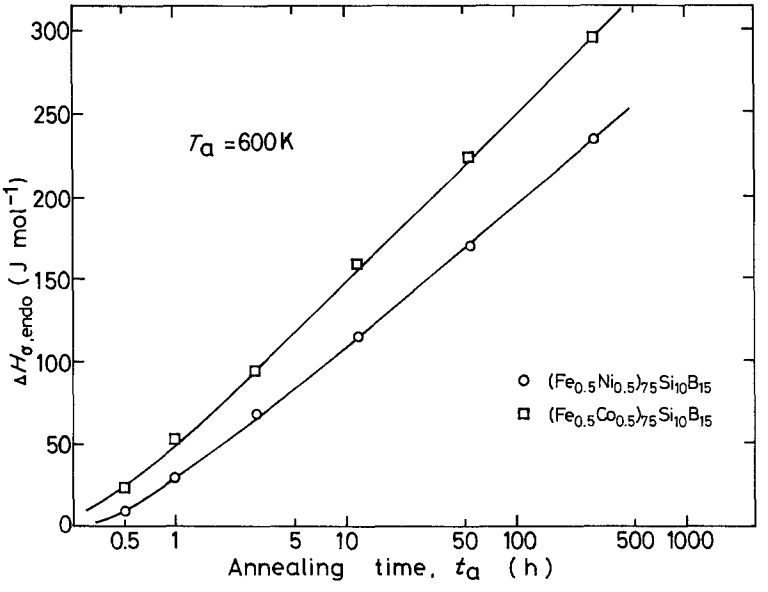

Figure 10 The variation of the enthalpy relaxation, $\Delta H_{\sigma,endo}$, as a function of annealing time, t_a, for amorphous $(Fe_{0.5}Ni_{0.5})_{75}Si_{10}B_{15}$ and $(Fe_{0.5}Co_{0.5})_{75}Si_{10}B_{15}$ alloys annealed at $T_a = 600$ K.

increase in the order Fe–Co > Fe–Ni > Co–Ni system. The $\Delta C_{p,max}$ and $\Delta H_{\sigma,endo}(600\,K)$ values of the ternary alloys decrease in the order Fe > Co > Ni. It is striking that the enthalpy relaxation is absent for the $Ni_{75}Si_{10}B_{15}$ amorphous alloy even after annealing for 200 h, similar to Pd–Ni–Si amorphous alloys in ribbons [25]. In the previous paper [25], we discussed the absence of ΔC_p in Pd–Ni–Si ribbon samples as being due to the precursory nuclei during annealing on the

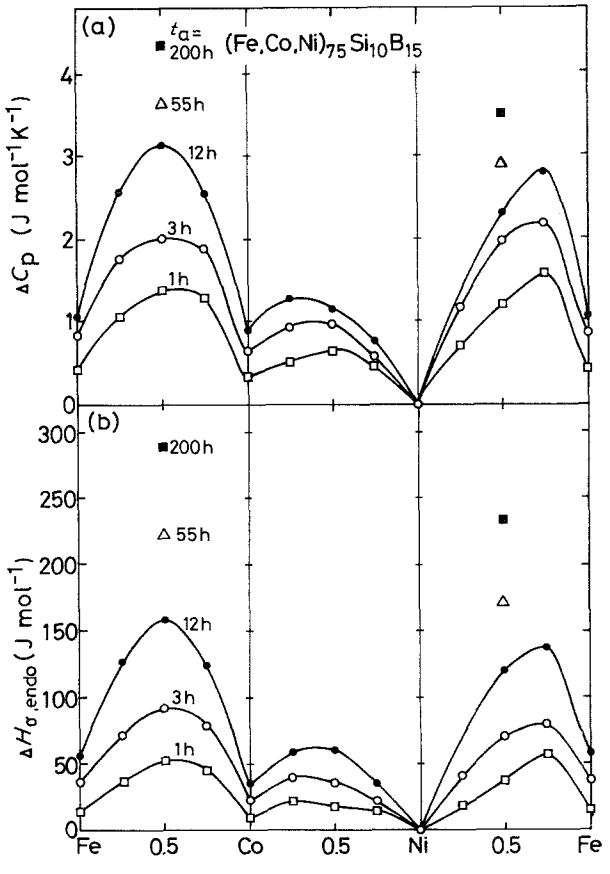

Figure 11 The composition dependences of the maximum differential specific heat, $\Delta C_{p,max}$ (a) and the enthalpy relaxation $\Delta H_{\sigma,endo}$ (b), for a series of (Fe, Co, Ni)$_{75}$Si$_{10}$B$_{15}$ amorphous alloys subjected to anneals at 600 K for different periods from 1 to 200 h.

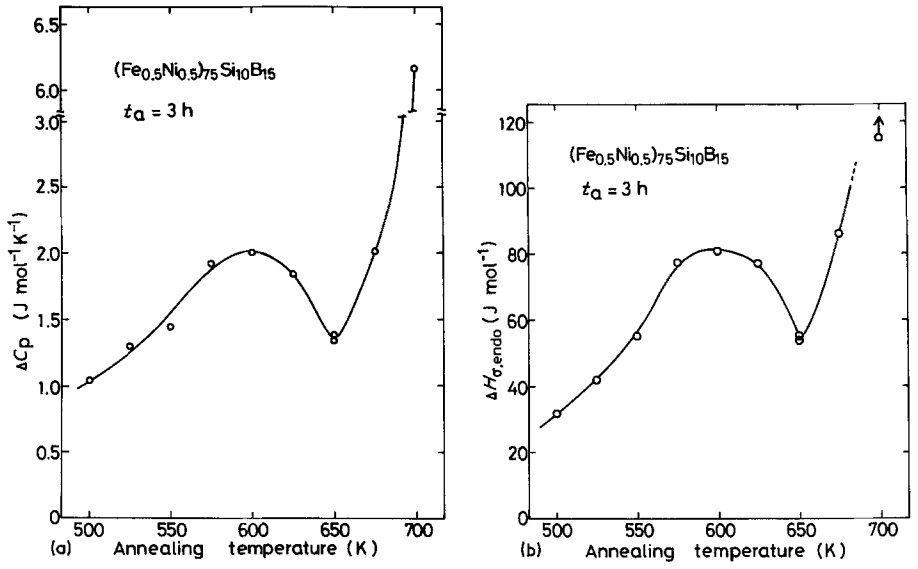

Figure 12 The variations of the maximum differential specific heat, $\Delta C_{p,max}$ (a) and the enthalpy relaxation $\Delta H_{\sigma,endo}$ (b) as a function of annealing temperature for an amorphous $(Fe_{0.5}Ni_{0.5})_{75}Si_{10}B_{15}$ alloy subjected to anneals for 3 h.

surface which grow on subsequent heating. Generation of the precursory nuclei during annealing on the surface leading to the disappearance of ΔC_p might be easy for the Ni–Si–B alloy in spite of the fact [31–33] that the $Ni_{75}Si_{10}B_{15}$ ternary alloy possesses an amorphous-forming ability much greater than those of $Co_{75}Si_{10}B_{15}$, $(Co–Fe)_{75}Si_{10}B_{15}$ and $(Co–Ni)_{75}Si_{10}B_{15}$ alloys, and the present ribbon thickness is much smaller than the critical ribbon thickness (170 μm) [31] for the formation of an amorphous single phase in $Ni_{75}Si_{10}B_{15}$ alloy. The problem of whether or not the absence of the endothermic effect in the Ni–Si–B alloy is an intrinsic phenomenon remains unanswered, but we believe that an extremely small structural change in the Ni–Si–B alloy leading to the excess endothermic reaction is another reason.

3.3. Changes in $\Delta C_{p,max}$ and $\Delta H_{\sigma,endo}$ with T_a

As an example, Fig. 12 shows the $\Delta C_{p,max} = C_p - C_{p,\nu}$ and $\Delta H_{\sigma,endo}$ values as a function of T_a for the $(Fe_{0.5}Ni_{0.5})_{75}Si_{10}B_{15}$ amorphous alloy after an anneal of $t_a = 3$ h. With increasing T_a, the values of both $\Delta C_{p,max}$ and $\Delta H_{\sigma,endo}$ initially increase, show maximum values at about 600 K, and then decrease significantly in the range from 600 to 650 K, followed by a rapid increase at temperatures slightly below T_g. The appearance of such two separate broad relaxation peaks is recognized for all other quaternary amorphous alloys used in the present work, suggesting that the enthalpy relaxation of $(Fe, Co, Ni)_{75}Si_{10}B_{15}$ alloys occurs by two distinguishable mechanisms. Accordingly, the annealing temperature range can be divided, for convenience, into the following two regions: (1) a sub-sub-T_g region in the range $T_a < T_g - 150$; and (2) a sub-T_g region in the range $T_g - 150 < T_a < T_g$. The magnitude of the enthalpy relaxation is much larger for the sub-T_g anneal than for the sub-sub-T_g anneal. The low-temperature enthalpy relaxation by the sub-sub-T_g anneal seems to be attributable to local and medium range atomic rearrangements, and the high-temperature relaxation by the sub-T_g anneal to the long-range cooperative atomic regroupings of an amorphous solid near T_g. In addition, Fig. 13 shows the temperature dependence of the difference in C_p between the as-quenched and the reference states, $\Delta C_p(T) = C_p(T) - C_{p,s}(T)$, for an amorphous $(Fe_{0.5}Ni_{0.5})_{75}Si_{10}B_{15}$ alloy. Two separate broad relaxation peaks are also seen in the ΔC_p–T relation; a low-temperature peak at about 600 K and a high-temperature peak at about 710 K. The appearance of two peaks in the ΔC_p–T relation for the as-quenched sample has been recognized in a number of amorphous alloys [34] and the structural relaxation of as-quenched samples upon continuous heating has been thought to occur by two distinct mechanisms of local atomic regroupings and cooperative atomic regroupings. From comparison of Figs. 12 and 13, one can easily notice a quite

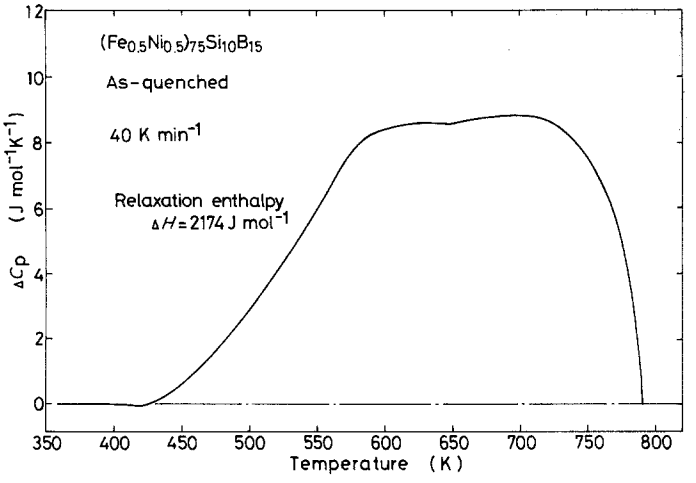

Figure 13 Difference in the apparent specific heat between the reference and as-quenched state, $\Delta C_p(T)$, for an amorphous $(Fe_{0.5}Ni_{0.5})_{75}Si_{10}B_{15}$ alloy.

good similarity between the $\Delta C_p(T)$ behaviour of the as-quenched sample and the $\Delta C_{p,max}(T_a)$ and $\Delta H_{\sigma,endo}(T_a)$ behaviour of the annealed samples; relaxation upon continuous heating and isochronal annealing occurs in two stages and the individual peak temperature is also almost the same. Therefore, two-stage enthalpy relaxations on annealing may be concluded to occur by local and medium range atomic rearrangements in the sub-sub-T_g anneal and by the long-range cooperative atomic regroupings in the sub-T_g anneal.

4. Discussion

4.1. Activation energy for enthalpy relaxation

If the ΔC_p peak at T_m is associated with a relaxation entity, an apparent activation energy for enthalpy relaxation, E_m, of the $(Fe_{0.5}Ni_{0.5})_{75}Si_{10}B_{15}$ amorphous alloy can be evaluated from isothermal annealing data of Fig. 3 using the following relation [22, 35]:

$$E_m(T_m)/k_B = \mathrm{d} \ln t_a^*/\mathrm{d}(1/T_a), \quad (4)$$

where t_a^* is the annealing time for the appearance of $\Delta C_{p,max}$ at T_m and k_B is Boltzmann's constant. Fig. 14 shows $\log t_a$ plotted against $1/T_a$ for the sub-sub-T_g (open circles) and the sub-T_g (solid circles) peaks of $(Fe_{0.5}Ni_{0.5})_{75}Si_{10}B_{15}$ amorphous samples. There exists a relatively good linear relation for each peak, indicating the satisfaction of an Arrhenius temperature dependence. It was found that $E_m(T_m)$ is not constant and increases with increasing T_m from 2.29 eV at $T_m = 620$ K to 3.15 eV at $T_m = 720$ K for the sub-sub-T_g peak and from 4.40 eV at $T_m = 720$ K to 4.96 eV at $T_m = 750$ K for the sub-T_g peak as shown in Fig. 15. Thus, the observed E_m increases significantly by the change of the sub-sub-T_g peak to the sub-T_g peak. The large $E_m(T_m)$ value in the sub-T_g range reflects the occurrence of cooperative structural relaxation.

4.2. Enthalpy relaxation spectra $H(E_m)$ and $H_o(E_m)$

In a previous section, the activation energy for enthalpy relaxation was found to exhibit a broad distribution. Chen [22] estimated the enthalpy relaxation spectrum as a function of E_m using Primak's theory [36] on the kinetics of processes distributed in activation energy. According to his analyses, the initial characteristic distribution $H(E_m)$ is given for an isothermal annealing at T_a after time t_a,

$$H(E_m) = \gamma(E_m)H_o(E_m) \simeq -(1/k_B T_a)(\mathrm{d}\Delta H_{\sigma,endo}/\mathrm{d} \ln t_a), \quad (5)$$

where $H_o(E_m)$ is the distribution of the relaxation entity, $\gamma(E_m)$ is the coupling strength contributing to the heat content $\Delta H_{\sigma,endo}$, and the activation energy, E_m, has the following relation to the frequency factor, ν_o, and T_m if one assumes the first order rate reaction process for the enthalpy relaxation:

$$E_m = k_B T_a \ln \nu_o t_a^* = k_B T_m \ln \nu_o \tau^* = E_m(T_m). \quad (6)$$

Here τ^* is the relaxation time at T_g and is related to the scanning rate $\alpha = 2/3\,\mathrm{K\,sec^{-1}}$ such that $\tau^* = k_B T_m^2/E_m\alpha \simeq 30$ sec. The frequency factor $\nu_o(T_m)$ calculated from Equation 6 increases with

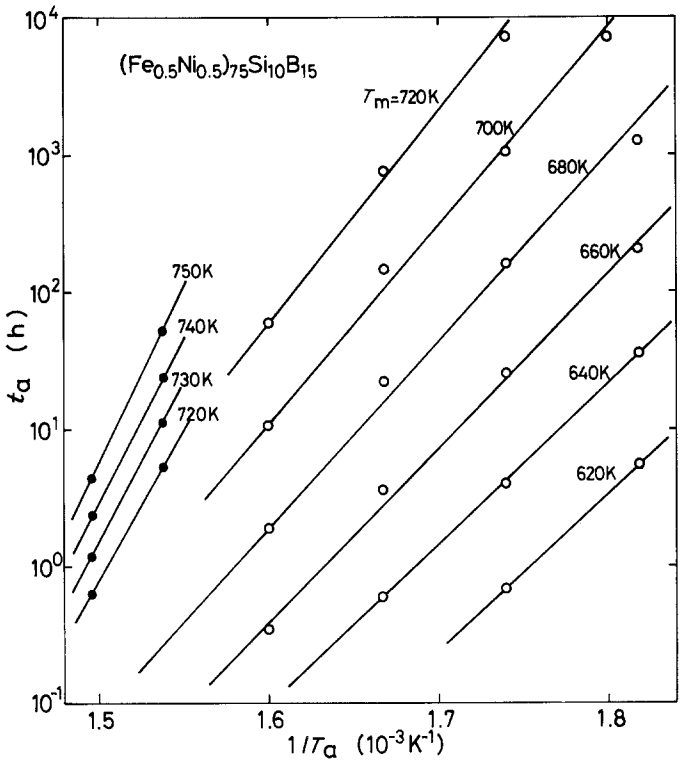

Figure 14 The annealing time, t_a^*, for the appearance of the ΔC_p peak at T_m as a function of the inverse of annealing temperature, $1/T_a$, for an amorphous $(Fe_{0.5}Ni_{0.5})_{75}Si_{10}B_{15}$ alloy.

T_m from $\simeq 10^{13}$ sec^{-1} at 620 K to $\simeq 10^{15}$ sec^{-1} at 720 K for the sub-sub-T_g reaction and from $\simeq 10^{21}$ sec^{-1} at 720 K to $\simeq 10^{23}$ sec^{-1} at 750 K for the sub-T_g reaction. These values of ν_o for the sub-sub-T_g reaction are somewhat higher than, but close to, the Debye frequency $\nu_D \simeq 10^{13}$ sec^{-1},

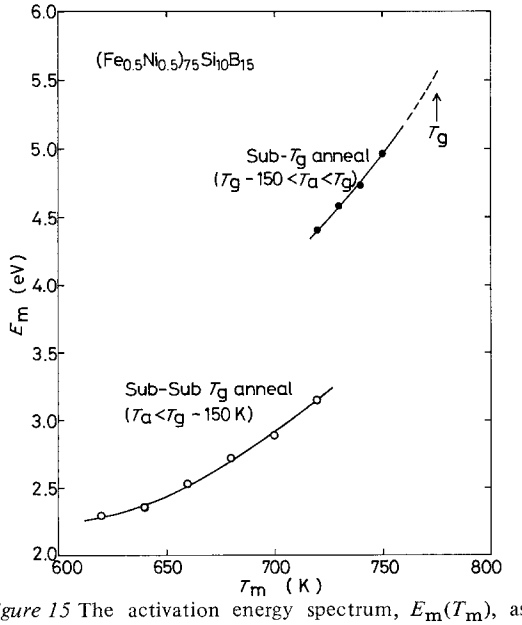

Figure 15 The activation energy spectrum, $E_m(T_m)$, as a function of T_m for an amorphous $(Fe_{0.5}Ni_{0.5})_{75}Si_{10}B_{15}$ alloy.

but those for the sub-T_g reaction are much higher than the ν_D value. $H(E_m)$ evaluated from the data of Figs. 10 and 15 are shown in Fig. 16a. Furthermore, $\Delta H_{\sigma,\text{endo}}$ can be approximated from Fig. 6 as $\Delta C_{p,\max}(T_m - T_a)$. As $\Delta C_{p,\max} \propto (T_m - T_a)^n$ with $n = 1$–2, and $dT_m/d \ln t_a \simeq 2 \times 10^{-2} T_a$ (see Fig. 3), Equation 7 reduces to

$$H(E_m) \simeq \frac{2\Delta C_{p,\max}}{k_B} \frac{dT_m/d\ln t_a}{T_a} \simeq (4\text{–}6) \times 10^{-2} \Delta C_{p,\max}/k_B. \quad (7)$$

One can see that $H(E_m)$ as a function of E_m shown in Fig. 16a reproduces fairly well the leading edge of the $\Delta C_p(T)$ curves.

In addition, Chen [22] reported that the unnormalized distribution spectrum is estimated from the relation $H_o^*(E_m) \simeq H(E_m)/(E_m - E_a)$, where E_a is the activation energy corresponding to T_a. The $H_o^*(E_m)$ values thus obtained are plotted in Fig. 16b and there is a clear tendency for the $H_o^*(E_m)$ to increase almost linearly with increasing E_m and T_m.

4.3. Interpretation of the enthalpy relaxation phenomenon

In the framework of a percolation process which has been conceived previously by Cohen and Grest

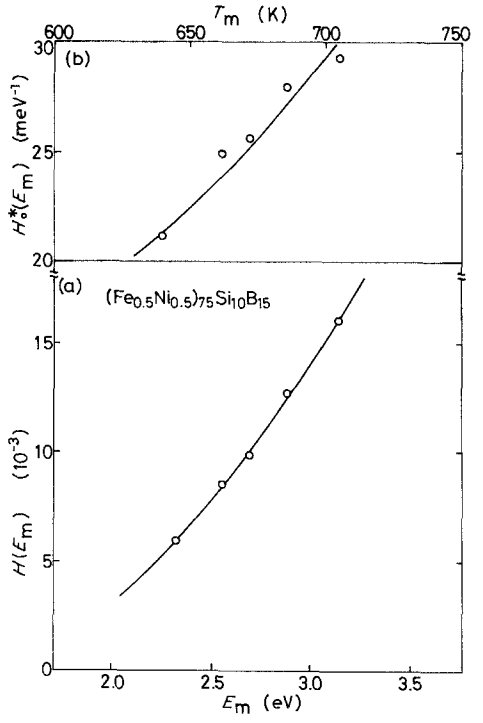

Figure 16 The enthalpy relaxation spectra $H(E_m)$ (a) and the unnormalized relaxation spectrum $H_o^*(E_m) \simeq H(E_m)/(E_m - E_a)$ (b), for an amorphous $(Fe_{0.5}Ni_{0.5})_{75}Si_{10}B_{15}$ alloy.

[37], Cyat [38] and Chen [22], we shall investigate the reason why the endothermic peak appears in the annealed samples. Cyat [38] and Chen [22] have proposed that a supercooled liquid structure near T_g is inhomogeneous and consists of liquid-like regions of large free volume or high local free energy and solid-like regions with small free volume or low local free energy. The resulting amorphous solid prepared by melt-quenching contains a number of liquid-like regions with unrelaxed atomic configuration which are isolated from each other, embedded in the relaxed solid-like matrix as illustrated in Fig. 17. The inhomogeneity for the present alloy systems is considered to arise from fluctuations in concentration and density. When the amorphous solid is annealed at T_a for t_a, part of the liquid-like regions undergo configurational change to a relaxed state by the independent and noncooperative manner. However, it may be emphasized that the local structural relaxation itself in the cluster involving several atoms can be cooperative. The sizes of the clusters can be approximated to be 1 to 2 nm. Each liquid-like region, m, manifests a liquid–amorphous transition at $T_{g,m}$ which depends on the atomic configuration state. The difference in specific heat, $\Delta C_{p,g}(T) = C_{p,s}(T) - C_{p,v}(T)$ (see Figs. 1 and 2) would then represent the distribution of the glass transition, $T_{g,m}$.

On annealing at temperatures well below T_g (sub-sub-T_g region), the regions with the relaxation times, τ_m, given by Equation 8, being shorter than the duration of annealing, t_a, would undergo local relaxations towards the local equilibrium states at T_a.

$$\tau_m \simeq \tau^* \exp\left[-\frac{\Delta\epsilon_m}{k_B}\left(\frac{1}{T_a} - \frac{1}{T_{g,m}}\right)\right], \quad (8)$$

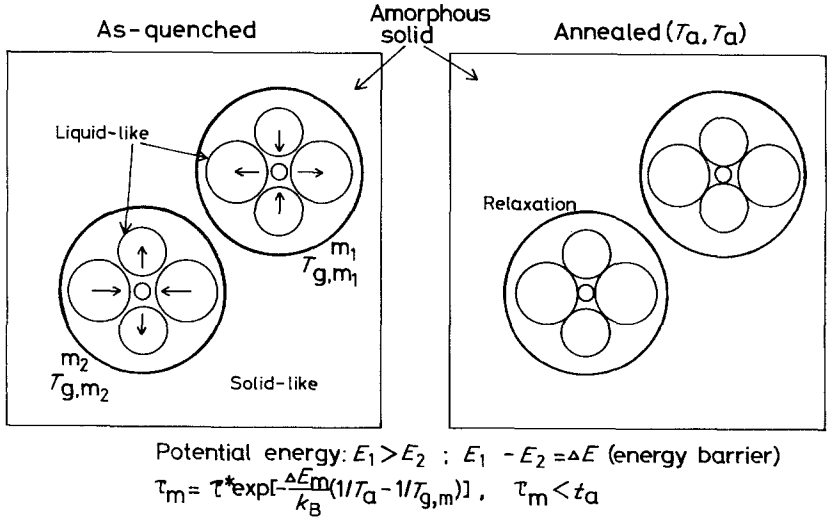

Figure 17 A schematic illustration showing the change in the as-quenched structure in a metal–metal–metalloid amorphous alloys with annealing at T_a for t_a.

where $\Delta\epsilon_m$ is the energy barrier between local potential minima. Each local relaxation contributes to the enthalpy relaxation proportional to $(T_{g,m} - T_a)$. Upon heating the annealed sample, each region, m, recovers the initial structure and contributes to an excess endothermic specific heat as the local amorphous–liquid transition occurs at or slightly above $T_{g,m}$. Thus both the temperature and intensity of the ΔC_p peak evolve in a continuous manner against the logarithm of t_a. The experimental activation energy spectrum $H_o^*(E_m)$ or $H_o^*(T_m)$ shown in Fig. 16b is fairly well analogous to the configurational specific distribution, $\Delta C_{p,g}$. It should be kept in mind that the energy barriers, $\Delta\epsilon_m$, are dependent on the local atomic configuration, or free volume, and hence the observed apparent activation energy $E_m(T_m)$ differs from $\Delta\epsilon_m$.

4.4. Reason for the significant composition effect on the enthalpy relaxation

In the investigation reported above, it was pointed out that the energy barrier for the endothermic reaction is dependent on the structural and compositional ordering and the more locally disordered configuration results in a smaller energy barrier ($\Delta\epsilon_m$). Accordingly, alloys exhibiting larger ΔC_p and $\Delta H_{\sigma,endo}$ values are thought to possess an amorphous structure with a higher degree of structural and compositional disorder. As a result, the number of the liquid-like (unrelaxed) regions with relaxation times shorter than the duration of annealing ($\tau_m < t_a$) increases, resulting in larger localized structural relaxation towards the local equilibrium states which contribute to an excess endothermic reaction in the recovery to the initial structure. Therefore, the degree of short-range structural and compositional disorder in the as-quenched state for a series of $(Fe, Co, Ni)_{75}Si_{10}B_{15}$ amorphous alloys may be noted to be the highest for $(Fe–Co)_{75}Si_{10}B_{15}$, followed by $(Fe–Ni)_{75}Si_{10}B_{15}$, $(Co–Ni)_{75}Si_{10}B_{15}$, $Fe_{75}Si_{10}B_{15}$, $Co_{75}Si_{10}B_{15}$ and then $Ni_{75}Si_{10}B_{15}$, suggesting that the admixture of different metal elements disturbs the formation of the short-range order, and the degree of disturbance tends to increase with increasing difference in ionic radius of the metal element itself. A large compositional effect on the magnitude of the ΔC_p peak has been also found for Pd–Ni–Si amorphous alloys [25]. It appears important to point out that a B_2O_3 glass [39] with a high degree of short-range order shows a small ΔC_p peak, and pronounced ΔC_p peaks are seen for polymeric glasses, polystyrene [40] and PVC [41].

4.5. Correlation between the enthalpy relaxation and the anneal-induced embrittlement

It is well known [42] that melt-quenched amorphous alloys undergo a marked loss in bending ductility on annealing at temperatures well below T_g and/or T_x (sub-sub-T_g region). One may expect the existence of a strong correlation between the local atomic rearrangements which contribute to the endothermic reaction in the sub-sub-T_g region and the low temperature anneal-induced embrittlement behaviour. Systematic information on the mutual relation for $(Fe, Co, Ni)_{75}Si_{10}B_{15}$ alloys is, however, missing even though the correlation for $Fe_{40}Ni_{40}P_{14}B_6$ and $(Fe_{0.5}Ni_{0.5})_{75}P_{16}B_6Al_3$ alloys has been investigated [44, 45]. Here we cite the data for the anneal-induced embrittlement for a series of amorphous $(Fe–Ni)_{78}Si_{10}B_{12}$ alloys which were reported previously by the present authors [43], even though there is a slight difference in boron content compared with the present alloy series. Fig. 18 shows changes in embrittlement parameters (T_o and a) as a function of nickel content for $(Fe–Ni)_{78}Si_{10}B_{12}$ amorphous alloys, together with the structure of the crystalline phase which appears first on crystallization. Here T_o is the annealing temperature at which the sample begins to fracture for the definite ageing time (60 sec), and a is the parameter representing the degree of embrittlement represented by $T_a'/\ln t_a'$ (T_a' is the annealing temperature at which the sample annealed for annealing time t_a' fractures), implying that the embrittlement tendency becomes large with lowering T_o and with increasing a_o. As seen in the figure, the embrittlement tendency of $(Fe_{1-x}Ni_x)_{78}Si_{10}B_{12}$ alloys is most pronounced around $x = 0.25$, and further replacement of iron by nickel inhibits the embrittlement. Although the boron content is 3 at% less than that of the present alloy series, it is reasonable to presume that the present $(Fe–Ni)_{75}Si_{10}B_{15}$ alloys exhibit a similar composition dependence of embrittlement as that of $(Fe–Ni)_{78}Si_{10}B_{12}$ alloys. When the magnitudes (Fig. 11) of $\Delta C_{p,max}$ and $\Delta H_{\sigma,endo}$ are compared with the embrittlement tendency shown in Fig. 18, one notices that the $(Fe_{0.75}Ni_{0.25})_{75}Si_{10}B_{15}$ alloy exhibiting the largest enthalpy relaxation possesses the largest embrittlement tendency.

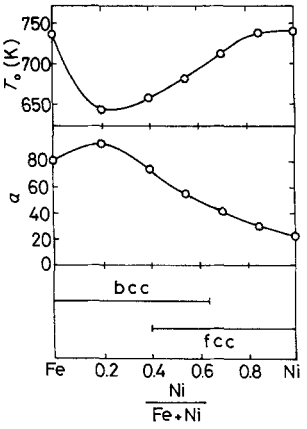

Figure 18 Changes in embrittlement parameters (T_o and a) and crystalline structure of MS-I phases of $(Fe–Ni)_{78}Si_{10}B_{12}$ amorphous alloys with nickel content. These data were taken from Inoue *et al.* [43].

In addition to the data on the composition dependence of the embrittlement for $(Fe–Ni)_{78}Si_{10}B_{12}$ alloys, our previous paper [43] pointed out that the anneal-induced embrittlement is more remarkable for Fe–Co–Si–B and Fe–Ni–Si–B alloys than for Co–Ni–Si–B alloys and that for the ternary alloys is most pronounced for Fe–Si–B, followed by Co–Si–B, and Ni–Si–B alloy which remains ductile even in partially crystalline state. A quite similar compositional effect on the embrittlement behaviour has been reported for a series of (Fe, Co, Ni)$_{75}P_{16}B_6Al_3$ amorphous alloys [46]. The composition dependences of the anneal-induced embrittlement described above correspond quite well to the ease with which the enthalpy relaxation occurs upon annealing and there exists a clear correlation that the larger the enthalpy relaxation the higher is the tendency for embrittlement. These results indicate that both the increase in the degree of short-range structural disorder in the as-quenched state, and the anneal-induced atomic rearrangements to the short-range structural and compositional ordering, result in an enhancement of the embrittlement tendency. The internal strain which generates by local atomic rearrangement is thought to become larger with the magnitude of the enthalpy relaxation, and the increase in the internal strain seems to be the cause of catastrophic loss of ductility.

Chen [46] has also pointed out that the enhancement of the anneal-induced embrittlement upon alloying is due to the enhanced phase separation and diffusivity caused by an increase in the excess configurational entropy of disorder upon alloying, and the larger the increase in the excess configurational entropy by alloying the larger is the embrittlement tendency. This also implies that the anneal-induced enthalpy relaxation is more remarkable in alloys exhibiting a large excess configurational entropy of mixing, i.e. a large degree of structural disorder in the as-quenched state where structural rearrangements upon annealing at elevated temperatures are more evident. The previous presumption is consistent with our new interpretation of the embrittlement mechanism of amorphous alloys derived from the data on the anneal-induced enthalpy relaxation.

5. Conclusions

In order to clarify the compositional effect on the anneal-induced enthalpy relaxation for (Fe, Co, Ni)$_{75}Si_{10}B_{15}$ amorphous alloys, structural relaxation behaviour was investigated calorimetrically for pre-annealed samples over a wide temperature range from well below to the glass transition temperature, T_g. The results obtained are:

1. upon heating the annealed samples, an excess endothermic reaction (enthalpy relaxation) occurs above the annealing temperature, T_a, indicative of an increase in the stability of the amorphous structure, and is followed by a broad exothermic reaction. The endothermic specific heat ΔC_p and the magnitude of the enthalpy relaxation $\Delta H_{\sigma,\mathrm{endo}}$ increase in a continuous manner with annealing time;

2. the annealing temperature dependence of the ΔC_p peak can be distinguished at two stages; a low temperature peak at approximately $T_g - 150\,K$, and a high temperature peak at a temperature slightly below T_g. The activation energy increases with increasing T_m from 2.29 eV at $T_m = 620\,K$ to 3.15 eV at $T_m = 720\,K$ for the sub-sub-T_g ($T_a < T_g - 150\,K$) relaxation and from 4.40 eV at 720 K to 4.96 eV at 750 K for the sub-T_g ($T_g - 150\,K < T_a < T_g$) relaxation. From these results, the endothermic reaction may be concluded to be due to the local and medium range atomic rearrangements for the low-temperature peak and to the long-range cooperative rearrangements for the high-temperature peak, by which each region recovers from relaxed configuration caused by annealing to unrelaxed initial structure;

3. the magnitude of the endothermic reaction (enthalpy relaxation) decreases in the order

Fe–Co > Fe–Ni > Co–Ni > Fe > Co and no ΔC_p peak is detected for the Ni–Si–B alloy. Such a significant composition dependence was thought to originate from the degree of short-range structural and compositional disorder in the as-quenched state; the alloy with higher short-range disorder exhibits a large enthalpy relaxation;

4. the concept of distribution in relaxation time, which had been previously conceived based on the percolation theory of glass transition, was found to be valid for the interpretation of the occurrence of reversible enthalpy relaxation with temperature in $(Fe, Co, Ni)_{75}Si_{10}B_{15}$ amorphous alloys and its significant composition dependence;

5. there exists a strong correlation that the alloys exhibiting a large enthalpy relaxation possess an enhanced tendency for embrittlement. The correlation is interpreted based on the assumption that the transition from the as-quenched disordered state to a relaxed equilibrium state causes a generation of internal strain, resulting in an enhancement of embrittlement.

References

1. H. S. CHEN, H. J. LEAMY and M. BARMATZ, *J. Non-Cryst. Solids* **5** (1971) 448.
2. M. BARMATZ and H. S. CHEN, *Phys. Rev.* **139** (1974) 4073.
3. B. S. BERRY and W. C. PRITCHER, *J. Appl. Phys.* **44** (1973) 3122.
4. H. S. CHEN and E. COLEMAN, *Appl. Phys. Lett.* **28** (1976) 245.
5. H. S. CHEN, *J. Appl. Phys.* **49** (1978) 4595.
6. T. EGAMI, *J. Mater. Sci.* **13** (1978) 2587.
7. Y. WASEDA and T. EGAMI, *ibid.* **14** (1979) 1249.
8. H. S. CHEN, R. C. SHERWOOD, H. J. LEAMY and E. M. GYORGY, *IEEE Trans. Mag.* **MAG-12** (1976) 933.
9. T. EGAMI, *Mater. Res. Bull.* **13** (1978) 557.
10. A. L. GREER and J. A. LEAKE, *J. Non-Cryst. Solids* **38-39** (1980) 379.
11. H. S. CHEN, *J. Appl. Phys.* **49** (1978) 3289.
12. A. KURSUMOVIC, M. G. SCOTT, E. GIRT and R. W. CAHN, *Scripta Metall.* **14** (1980) 1303.
13. B. FOGARASSY, A. BOHONYEI, A. CZIRAKI, I. SZABO, GY. FAIGEL, L. GRANASY, T. KEMENY and I. VINCZE, *J. Non-Cryst. Solids* **61/62** (1984) 907.
14. M. BALANZAT, *Scripta Metall.* **14** (1980) 173.
15. E. BALANZAT, C. MAIVY and J. HILLARET, *J. Phys.* **C-8** (1980) 871.
16. A. J. DREHMAN and W. L. JOHNSON, *Phys. Status Solidi (a)* **52** (1979) 499.
17. A. RAVEX, J. C. LASJAUNIAS and O. BETHOUX, *Physica* **107B** (1981) 397.
18. C. C. KOCH, D. M. KROEGER, J. S. LIN, J. O. SCARBROUGH, W. L. JOHNSON and A. C. ANDERSON, *Phys. Rev.* **27** (1983) 1586.
19. A. INOUE, S. OKAMOTO, N. TOYOTA, T. FUKASE, K. MATSUZAKI and T. MASUMOTO, *J. Mater. Sci.* **19** (1984) in press.
20. J. W. DRIJVER, A. L. MULDER, W. C. EMMES and S. RADELAAR, "Rapidly Quenched Metals III", Vol. 1, edited by B. Cantor (The Metals Society, London, 1978 p. 363.
21. H. S. CHEN, *J. Appl. Phys.* **52** (1981) 1868.
22. *Idem, J. Non-Cryst. Solids* **46** (1981) 289.
23. *Idem*, "Proceedings of the 4th International Conference on Rapidly Quenched Metals", edited by T. Masumoto and K. Suzuki (Japan Institute of Metals, Sendai, 1982) p. 495.
24. J. W. DRIJVER, A. L. MULDER and S. RADELAAR, *ibid.*, p. 535.
25. H. S. CHEN and A. INOUE, *J. Non-Cryst. Solids* **61/62** (1984) 805.
26. D. SROLOVITZ, K. MAEDA, V. VITEK and T. EGAMI, *Phil. Mag.* **A44** (1981) 847.
27. S. KOBAYASHI and H. TAKEUCHI, "Proceedings of the 4th International Conference on Rapidly Quenched Metals", edited by T. Masumoto and K. Suzuki (Japan Institute of Metals, Sendai, 1982) p. 505.
28. A. J. KAVACS, *Fotchr. Hochpolym-Forsch* **3** (1963) 394.
29. H. S. CHEN, *J. Appl. Phys.* **49** (1978) 4595.
30. R. SUZUKI, K. SHIBUE, K. OSAMURA, P. H. SHINGU, Y. MURAKAMI, *J. Mater. Sci. Lett.* **1** (1982) 127.
31. M. HAGIWARA, A. INOUE and T. MASUMOTO, *Met. Trans.* **12A** (1981) 1027.
32. M. HAGIWARA, A. INOUE and T. MASUMOTO, *Sci. Rep. Res. Inst. Tohoku Univ.* **A29** (1981) 351.
33. M. HAGIWARA, A. INOUE and T. MASUMOTO, *Mater. Sci. Eng.* **54** (1982) 197.
34. H. S. CHEN and E. COLEMAN, *Appl. Phys. Lett.* **28** (1976) 245.
35. H. S. CHEN, *J. Non-Cryst. Solids* **27** (1978) 257.
36. W. PRIMAK, *Phys. Rev.* **100** (1955) 1677.
37. M. H. COHEN and G. S. GREST, *ibid.* **B20** (1979) 1077.
38. M. CYAT, *J. Phys.* **C8** (1980) 107.
39. H. S. CHEN and C. R. KURKJIAN, *J. Amer. Ceram. Soc.* **66** (1983) 613.
40. H. S. CHEN and T. T. WANG, *J. Appl. Phys.* **52** (1981) 5898.
41. A. R. BERENS and I. M. HODGE, *Macromolecules* **15** (1982) 756.
42. H. S. CHEN, *Rep. Prog. Phys.* **43** (1980) 353.
43. A. INOUE, H. M. KIMURA and T. MASUMOTO, *J. Japan Inst. Metals* **42** (1978) 303.
44. *Idem, Sci. Rep. Res. Inst. Tohoku Univ.* **A27** (1979) 159.
45. H. S. CHEN, "Proceedings of the 4th International Conference on Rapidly Quenched Metals", edited by T. Masumoto and K. Suzuki (Japan Institute of Metals, Sendai, 1982) p. 555.
46. *Idem, Mater. Sci. Eng.* **26** (1976) 79.

Received 20 January
and accepted 30 January 1984